Electrochromic materials using mechanically interlocked molecules

2008 Sci. Technol. Adv. Mater. 9 014104

(http://iopscience.iop.org/1468-6996/9/1/014104)

IOP PUBLISHING SCIENCE AND TECHNOLOGY OF ADVANCED MATERIALS

Sci. Technol. Adv. Mater. **9** (2008) 014104 (7pp) doi:10.1088/1468-6996/9/1/014104

TOPICAL REVIEW

Electrochromic materials using mechanically interlocked molecules*

Taichi Ikeda[1] **and James Fraser Stoddart**[2]

[1] Functional Modules Group, Organic Nanomaterials Center, National Institute for Materials Science, 1-1 Namiki, Tsukuba, Ibaraki, 305-0044, Japan
[2] The California NanoSystems Institute and Department of Chemistry and Biochemistry, University of California, Los Angeles, 405 Hilgard Avenue, Los Angeles, CA 90095-1569, USA

E-mail: stoddart@chem.ucla.edu

Received 22 October 2007
Accepted for publication 7 January 2008
Published 13 March 2008
Online at stacks.iop.org/STAM/9/014104

Abstract
Recent investigations on the design and synthesis of electrochromic materials based on switchable three-station [2]catenanes are summarized. The reasoning and preliminary experiments behind the design of electrochemically controllable red–green–blue (RGB), donor–acceptor [2]catenanes are presented. A basis for color generation is discussed in which the tetracationic cyclophane, cyclobis(paraquat-*p*-phenylene), serves as the π-electron deficient ring which circumrotates between three π-electron rich recognition sites within a macrocyclic polyether, generating the three different colors (RGB) based on the different charge transfer interactions between the tetracationic cyclophane and recognition sites based on 1,5-dioxynaphthalene (R), tetrathiafulvalene (G) and benzidine (B). Issues relating to the realization of an RGB [2]catenane are raised and discussed: they include (i) color tuning, (ii) thermodynamic considerations, (iii) electrochemistry on model compounds, (iv) molecular design, (v) the electrochemical behavior of three-station [2]catenanes and (vi) electrochromism in polymer gel matrices. Finally, the challenges that need to be met in the future if the ideal RGB catenane is to be prepared, are outlined.

Keywords: interlocked molecules, [2]catenanes, electrochromism, carge-transfer complex, electronic paper display

(Some figures in this article are in colour only in the electronic version.)

1. Introduction

Advances in information technology are accelerating the development of novel organic materials [1, 2]. These organic materials have been proposed as alternatives to inorganic materials. They could lead to thin, flexible and lightweight portable devices, capable of accessing information anywhere, so-called 'ubiquitous computing' [3]. Electronic paper displays (E-PADs) are devices which promise to change our life style. The concept of an E-PAD, a low-cost and reflective display that feels like a document printed on conventional paper, emerged as an idea in the late 1990 s [4]. Several prototypes of pixel components in the E-PADs have been demonstrated, e.g. electrophoresis of the colored particle in the capsules [5, 6], liquid crystals [7, 8], and electrochromism [9, 10]. Recently, we have proposed mechanically interlocked molecules as a different and unique kind of the electrochromic materials [11]. Mechanically interlocked compounds [12] which consist of a pair of mutually interlocked ring components are referred to as [2] catenanes. The interlocked donor–acceptor compounds

* Invited paper.

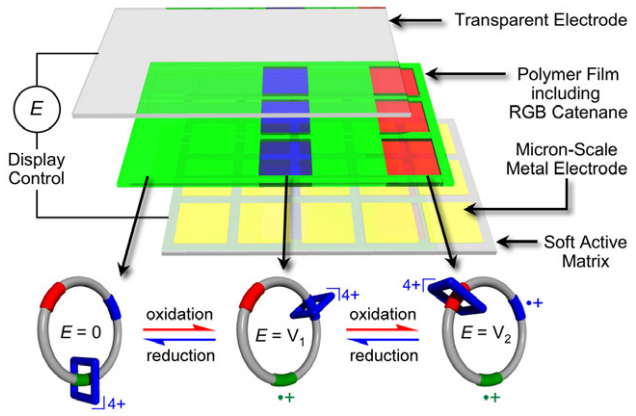

Figure 1. The proposed design for electronic paper display (E-PAD) based on the electrochromism of electrochemically-controllable three-station [2]catenanes. The control voltage is applied between the transparent electrode and the soft active matrix to manipulate the three-station [2]catenanes which are capable of exhibiting RGB colors in response to the applied voltage. The RGB colors originate from the CT absorption bands between the tetracationic cyclophane and the three stations on the macrocyclic polyethers.

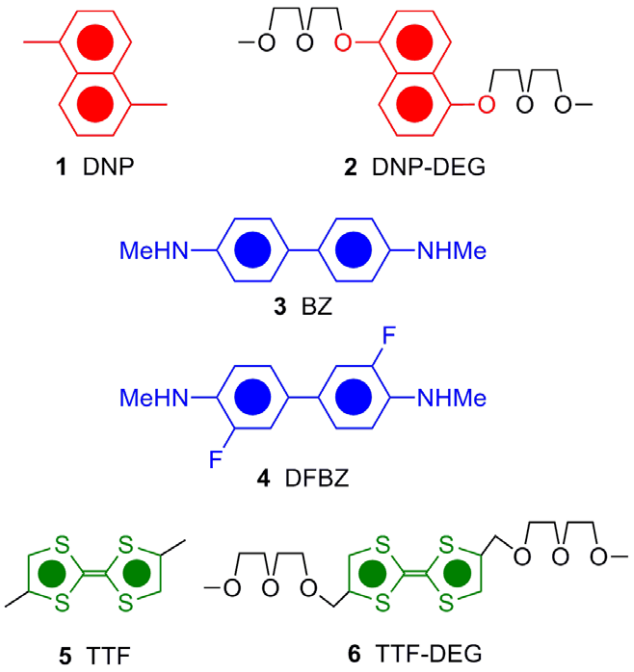

Figure 2. Structural formulae of the series of model guests **1**–**6** DNP, DNP–DEG, BZ, DFBZ, TTF and TTF–DEG for DFT calculation.

[13–15] we have been developing in recent years in the shape of two-station [2]catenanes [16–19] are usually composed of the π-electron deficient tetracationic cyclophane, cyclobis(paraquat-*p*-phenylene) ($CBPQT^{4+}$) [20–23], and another π-electron rich ring, encompassing multiple binding sites (stations) for the $CBPQT^{4+}$ ring—for instance, tetrathiafulvalene (TTF) [24–26], 1,5-dioxynaphthalene (DNP) [27–29] and benzidine (BZ) [30, 31], etc. When the π-electron deficient $CBPQT^{4+}$ ring resides on a π-electron rich binding site, the compound exhibits the color on account of charge-transfer (CT) between the $CBPQT^{4+}$ ring and the binding site [20–31]. In the case of the two-station [2]catenanes, we have designed an electrochemically controllable one, where the $CBPQT^{4+}$ ring resides preferentially at one or another binding sites in the ground and electrochemically oxidized states, respectively. We can observe the electrochromism in response to the circumrotation of the $CBPQT^{4+}$ ring from one binding site to another [32–34]. Based on these findings, we have suggested that electrochemically controllable red–green–blue (RGB) [2]catenanes could be the basis (figure 1) for constructing different kinds of electrochromic devices [11]. In such a system, we might expect that a change in the location of the $CBPQT^{4+}$ ring between the three π-electron rich stations might generate three different colors (RGB) based on the different CT interactions between the $CBPQT^{4+}$ ring and the three distinct, carefully chosen stations. Compared to the other prototypes of E-PADs, the advantages in using RGB [2]catenane are as follows: (i) Each pixel unit needs only a single basic cell instead of three to generate the red, green, and blue colors. This feature would reduce dramatically the complexity and, hence, the cost of electrochromic devices. (ii) Molecular compounds are easily embedded in polymer matrices [34] and even on paper as well. Thus, simple package processing, such as ink-jet printing technology, could be used to manufacture the display.

In this review, we summarize our recent investigations on electrochromic materials using mechanically interlocked molecules. We discuss several issues in trying to achieve an RGB [2]catenane including: (i) color tuning, (ii) thermodynamics, (iii) electrochemistry, (iv) molecular design, (v) electrochemical properties of three-station [2]catenanes and (vi) electrochromism in polymer gel matrices. Furthermore, we highlight some issues that need to be tackled in the future.

2. Color tuning

DFT calculations help in choosing the host–guest pairs for RGB colors. The color of donor–acceptor [2]catenanes arises from the CT band between the HOMO of aromatic crown ethers and the LUMO of $CBPQT^{4+}$. We have calculated the CT band gap energy between the tetracationic cyclophane, $CBPQT^{4+}$, and the model guest compounds **1**−**6** (figure 2) [11]. The results of the calculations are summarized in table 1. The DFT calculations predicted that DNP–DEG, TTF–DEG and DFBZ should be ideal guest molecules to obtain the RGB colors. Based on this prediction, we synthesized some model compounds **7**−**11** (figure 3) [35, 36]. Figure 4 shows the UV-Vis spectra of the $CBPQT^{4+}$ inclusion complex in MeCN. The absorption maxima of the $CBPQT^{4+}$ complexes with DNP–TEG, DFBZ–TEG and TTF–TEG are 525, 610 and 835 nm, respectively. The inset in figure 4 reveals that we obtained RGB colors from these three combinations.

3. Thermodynamics

The binding strengths of the model guests **7**−**11** with the $CBPQT^{4+}$ [35, 36] were obtained from measurements

Table 1. The CT band gap energy (ΔE_{CT}) between the HOMO of the guest and the LUMO of CBPQT^{4+} • 4PF$_6$ and absorption maxima (λ_{max}) of the CT band obtained from DFT calculations [a] and the experiments.

	1 DNP	**2** DNP–DEG	**3** BZ	**4** DFBZ	**5** TTF	**6** TTF–DEG
calc. E_{CT} (eV) [b]	2.68	2.60	1.82	2.06	1.46	1.64
calc. λ_{max} (nm) [c]	462	476	677	601	853	756
obs. λ_{max} (nm) [d]	473	525	670	–	854	835

[a]B3LYP/66-3 ** + + level based on the structure optimized using B3LYP/6-331G *.
[b]The band gap energy of CT band calculated by DFT.
[c]The absorption maxima of the CT band calculated from ΔE_{CT}.
[d]The absorption maxima of the CT band obtained from the experiment.

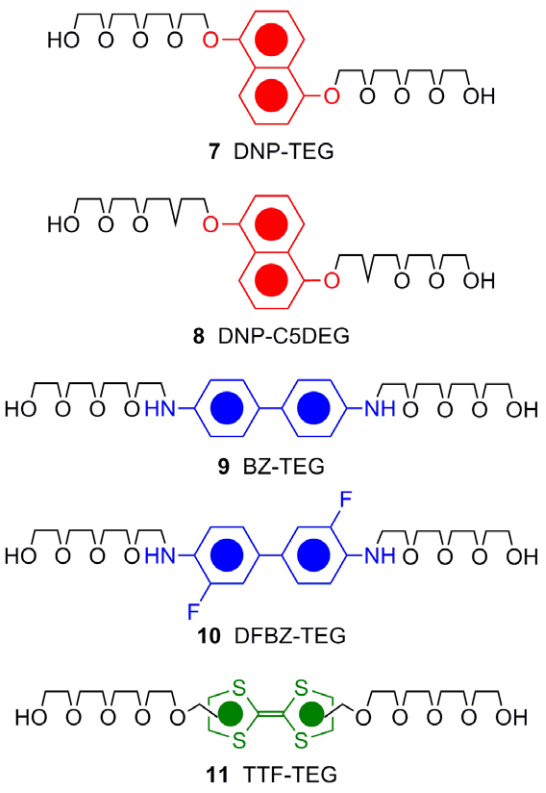

Figure 3. Structural formulae of the series of model guests **7–11** DNP–TEG, DNP–C5DEG, BZ–TEG, DFBZ–TEG, TTF–TEG.

carried out in MeCN solutions by isothermal titration calorimetry (ITC). The thermodynamic data are summarized in table 2. Of all these model guests, TTF–TEG has the largest association constant ($K_a = 416 \times 10^3\,M^{-1}$) with the CBPQT^{4+}. DNP–TEG is the second largest ($K_a = 43.9 \times 10^3\,M^{-1}$). In the case of DNP–C5DEG, it is evident that the simple modification, where the second closest oxygen atoms from the naphthalene ring were replaced by methylene groups, drastically reduces the binding affinity to CBPQT^{4+} [35]. X-Ray crystallographic data for the 1 : 1 complex formed between DNP–TEG and CBPQT^{4+} indicates that the second closest oxygen atoms from the naphthalene ring are involved in [CH • • • O] interactions with the CBPQT^{4+} ring [27–29]. In the case of the DNP–C5DEG, the absence of oxygen

Table 2. The thermodynamic binding data corresponding to the complexation between CBPQT • 4PF$_6$ and the model compounds **7–11** in MeCN determined by ITC at 298 K.

Guest	H[a] (kJ mol^{-1})	TS[b] (kJ mol^{-1})	G[c] (kJ mol^{-1})	K_a[d] ($\times 10^3$ M^{-1})
7, DNP–TEG	-65.4 ± 0.2	-38.8	-26.5	43.9 ± 0.8
8, DNP–C5DEG	-57.3 ± 0.3	-45.3	-11.9	0.122 ± 0.001
9, BZ–TEG	-42.3 ± 1.0	-23.6	-18.7	1.91 ± 0.09
10, DFBZ–TEG	-51.6 ± 0.3	-37.3	-14.2	0.312 ± 0.003
11, TTF–TEG	-60.9 ± 0.2	-28.7	-32.1	416 ± 23

[a]Enthalpy change of the reaction.
[b]Calculated from the H and G values by using the equation $G = H - TS$.
[c]Calculated from the fitted value of K_a by using the equation $G = -RT\ln K_a$.
[d]Obtained from curve-fitting to the binding isotherm. Fits were performed with the software provide by Mecrocal LLC, and the stoichiometry of all complexes was between 0.97 and 1.03, indicating that a 1 : 1 complex was formed.

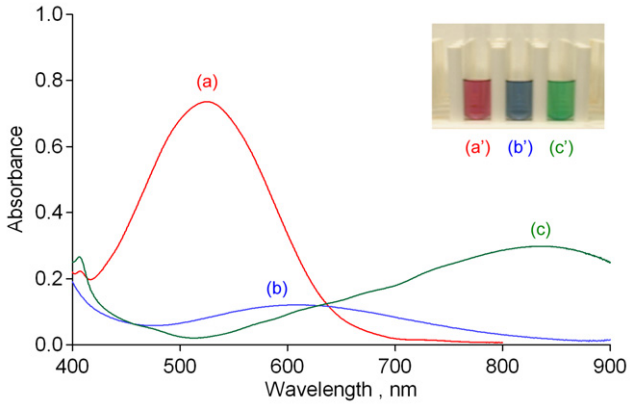

Figure 4. UV-Vis spectra of the CBPQT^{4+} inclusion complexes with (a) DNP–TEG (1 mM), (b) BZ–TEG (1 mM), and (c) TTF–TEG (0.1 mM). A photograph of the CBPQT^{4+} inclusion complexes (a′) DNP–TEG, (b′) BZ–TEG and (c′) TTF–TEG is shown as an inset.

atoms to form [CH • • • O] interactions results in a much reduced binding affinity. The K_a value ($1.91 \times 10^3\,M^{-1}$) for DFBZ–TEG is much smaller than that ($0.312 \times 10^3\,M^{-1}$) of BZ–TEG, presumably because of the detrimental effect that the fluorine atoms have, both electronically and sterically, on the binding of a BZ unit inside the CBPQT^{4+} cavity [36].

4. Electrochemistry

Electrochemistry on the model compounds **7** and **9**−**11** was performed using cyclic voltammetry (CV) and differential pulse voltammetry (DPV) [35, 36]. The half-wave potentials ($E_{1/2}$) were determined from the DPV peals. The $E_{1/2}$ values are summarized in table 3. DNP–TEG shows a quasi-reversible redox process and it has the largest $E_{1/2}$ value [33, 35]. TTF–TEG shows a reversible redox process and it has the smallest $E_{1/2}$ value [25, 33, 35]. Both BZ–TEG [30, 31] and DFBZ–TEG [36] exhibit reversible redox processes and their $E_{1/2}$ values lie between those of TTF–TEG and DNP–TEG.

Table 3. Electrochemical data for the model compounds [a].

	Oxidation (V)	Reduction (V)
7, DNP–TEG	+1.16	
9, BZ–TEG	+0.46, +0.65	
10, DFBZ–TEG	+0.65, +0.83	
11, TTF–TEG	+0.36, +0.71	
CBPQT•4PF$_6$		−0.29, −0.72

[a]Argon-purged MeCN, room termperature, 0.1 M TBA • PF$_6$ as supporting electrolyte. Working electrode: glassy carbon. Counter electrode: Pt wire. Reference electrode: saturated calmel electrode.

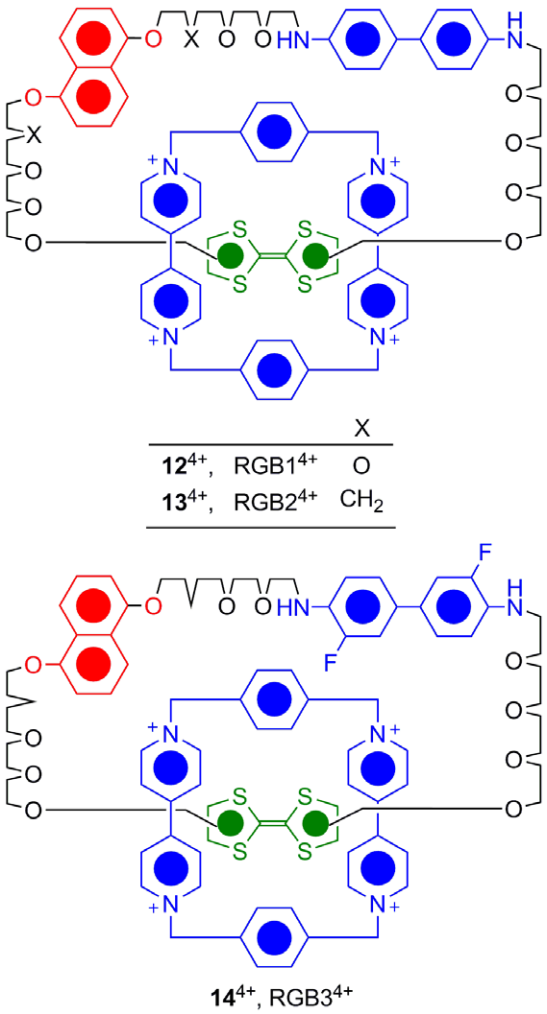

Figure 5. Structural formulae of the first, second and third generation RGB [2]catenanes **12**$^{4+}$–**14**$^{4+}$.

5. Molecular design

Based on our preliminary investigations, we were led to propose the design of the RGB catenanes illustrated in figure 5 [11, 35]. In the first generation RGB catenane (**12**$^{4+}$, RGB1^{4+}), the three stations—TTF diol, BZ and DNP—were simply linked by oligoethyleneglycol chains. In the second generation RGB catenane (13^{4+}, RGB2^{4+}), the second closest oxygen atoms from the naphthalene ring were substituted by methylene groups. In other words, the three stations—TTF diol, BZ and DNPC5DEG—were linked by oligoethyleneglycol chains. In the third generation RGB catenane (14^{4+}RGB3^{4+}), the three stations—TTF diol, DFBZ and DNPC5DEG—were also linked by the oligoethyleneglycol chains. We have already synthesized the RGB1^{4+} and RGB2^{4+} [17]

Table 4. DPV peak potentials versus SCE (V) for RGB1•4PF$_6$ and RGB2•4PF$_6$[a].

Compound	Scan direction	DPV peak top potential [b]
RGB1•4PF$_6$	Anodic	+0.39, +0.49, +0.71
	Cathodic	+0.38, +0.49, +0.71
RGB2•4PF$_6$	Anodic	+0.48, +0.58, +0.70
	Cathodic	+0.53, +0.70

[a]Argon-purged MeCN, room temperature, 0.1 M TBA•PF$_6$ as supporting electrolyte. Working electrode: glassy carbon. Counter electrode: Pt wire. Reference electrode: saturated calomel electrode.
[b]The relation between the peak potential in the DPV measurement (E_{max}), half-wave potential ($E_{1/2}$), and pulse height ($E = 25$ mV) is ($E_{1/2} = E_{max} + E/2$.

6. Electromechanical behavior of RGB1^{4+} and RGB2^{4+}

The electrochemical properties of the RGB [2] catenanes RGB1^{4+} and RGB2^{4+} were investigated by CV and DPV [17]. Interestingly, CV and DPV peaks were different in the anodic and cathodic scans, an observation which is attributable to the electromechanical movement of the interlocked CBPQT^{4+} ring on the polyether macrocycle [33]. Table 4 summarizes the DPV peak potentials of the three-station [2]catenanes RGB1^{4+} and RGB2^{4+}. Each peak was assignable using the spectroelectrochemistry [35]. Based on the results of thermodynamics, electrochemistry and spectroelectrochemistry, we established the electromechanical behavior of the three-station [2]catenanes RGB1^{4+} (scheme 1) and RGB2^{4+} (scheme 2) [35]. In the anodic scan of the RGB1^{4+}, a small DPV peak was observed at +0.39 V. This oxidation has been assigned to the oxidation of the unoccupied TTF [state (i′) → (ii)] [25, 33]. In the case of the RGB1^{4+}, there is an equilibrium between the states (*i′*) and (i). The oxidations of the occupied TTF and the BZ units take place at almost the same potential ($E = +0.50$ V)[state (i) → (ii) → (iii)]. The TTF radical cation repels the CBPQT^{4+} ring by Coulombic repulsion [32, 33]. This translocation of the CBPQT^{4+} ring was confirmed by means of spectroelectrochemistry. The association constants for complexation of DNP–TEG and BZ–TEG ($K_a = 43.9 \times 10^3$ M^{-1}, 1.91×10^3 M^{-1}, respectively) with CBPQT•4PF$_6$ suggest the CBPQT^{4+} ring resides on the DNP station preferentially [state (ii)]. Further oxidations from the radical cations to the dications occurs at +0.72 V[state (iii) → (iv)]. This process is reversible. After the reduction of the BZ radical cation at +0.50 V[state (iii) → (ii)], the reduction of the TTF radical cation takes place at +0.39 V. This potential is almost the same one as that for the oxidation of an unoccupied TTF, an observation which implies that the CBPQT^{4+} ring does not reside on the TTF radical

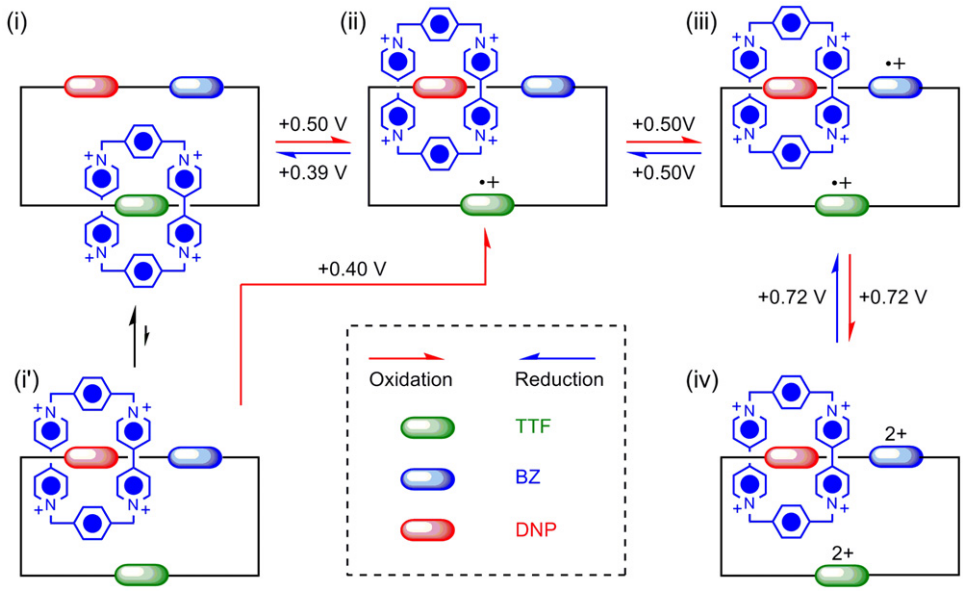

Scheme 1. Expected electromechanical behavior of the three-station [2]catenane **RGB1** • $4PF_6$. In the ground state, **RGB1** • $4PF_6$ is in equilibrium between states (i) and (i′). The red and blue arrows represent the oxidation and reduction processes, respectively.

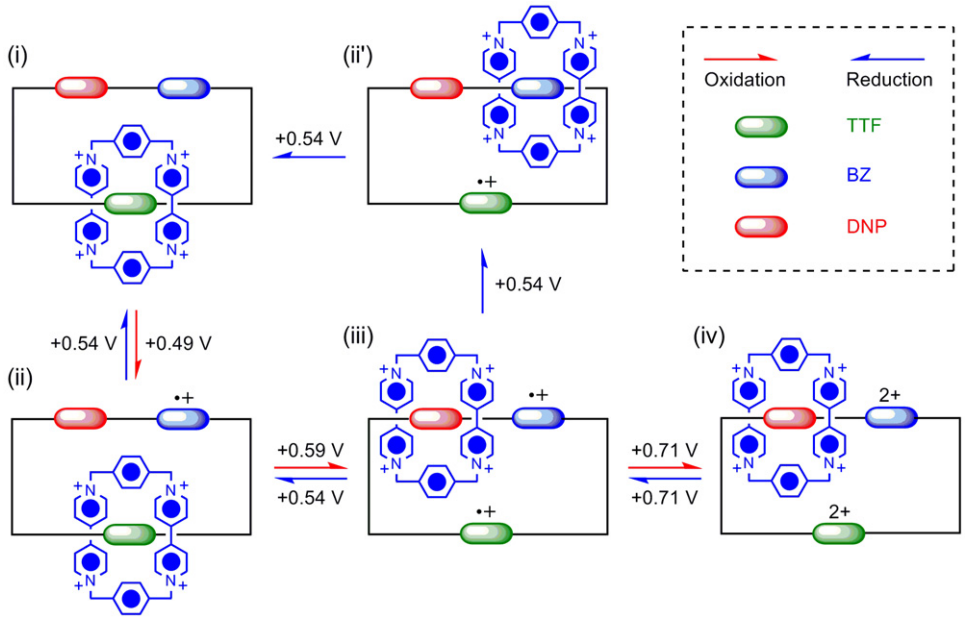

Scheme 2. Expected electromechanical behavior of **RGB2** • $4PF_6$. The red and blue arrows represent the oxidation and reduction processes, respectively. As the reduction potentials of the $TTF^{\bullet+}$ and $BZ^{\bullet+}$ radical cations are almost the same, two reduction processes can be proposed: (iii) → (ii) → (i) and (iii) → (ii′) → (i). In the latter case, the $CBPQT^{4+}$ ring visits all of the three stations.

cation [state (ii)]. Overall, we have not been able to determine a state in which the $CBPQT^{4+}$ ring resides preferentially on the BZ unit. As a consequence, we conclude that the three-station [2]catenane $RGB1^{4+}$ is, in reality, a bistable entity.

In the anodic scan of the $RGB2^{4+}$, the first oxidation takes place at the BZ unit at +0.49 V[state (i) → (ii)]. As could be predicted from the association constant ($K_a = 122\,M^{-1}$) between $CBPQT^{4+}$ • $4PF_6$ and DNP–C5DEG, the association of the $CBPQT^{4+}$ ring with the DNP unit is quite weak in this [2]catenane. Thus, the $CBPQT^{4+}$ ring resides almost exclusively on the TTF unit and inhibits the first oxidation of the TTF unit. The occupied TTF unit is oxidized at +0.59 V[state (ii) → (iii)]. This step is accompanied by the translocation of the $CBPQT^{4+}$ ring to the neutral DNP unit. Then, the TTF and BZ radical cations are oxidized to the dications at +0.71 V[state (iii) → (iv)]. This process is reversible. In the cathodic scan, the reductions of the TTF and BZ radical cations take place at similar potentials ($E = +0.54$ V). In some molecules, the reduction of the BZ radical cation occurs before that of the TTF radical cation. In such a case, the $CBPQT^{4+}$ ring resides preferentially on the neutral BZ unit [state (iii)→(ii′)→(i)]. In other molecules, another route might well be followed [state (iii) → (ii) → (i)]. In the former route, the $CBPQT^{4+}$

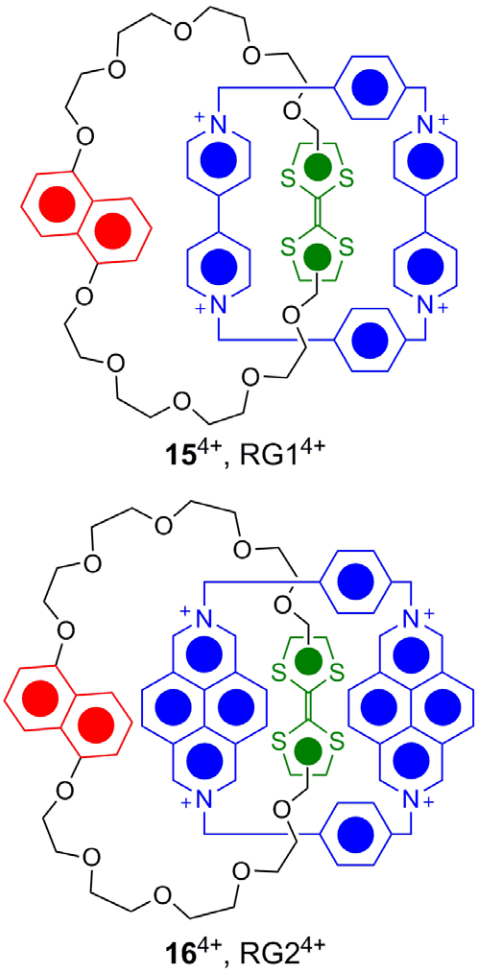

Figure 6. Structural formulae of the first, second and third generation RG [2]catenanes $\mathbf{15}^{4+}$ and $\mathbf{16}^{4+}$

ring visits all of the three stations. Taking the half-wave potentials $[E_{1/2}(\mathrm{TTF}-\mathrm{TEG}) < E_{1/2}(\mathrm{BZ}-\mathrm{TEG})]$ of TTF–TEG and BZ–TEG into account, the former route may be the major one. We are, therefore, led to the conclusion that the three-station [2]catenane $\mathrm{RGB2}^{4+}$ is a quasi-tristable [2]catenane [35].

7. Electrochromism in polymer gel matrix

The electrochromism of the two-station [2]catenanes $\mathrm{RG1}^{4+}$ and $\mathrm{RG2}^{4+}$ (figure 6) in a polymer gel matrix (polymethylmethacrylate gel) has been observed [34]. The kinetics of the electrochromism were obtained from CV measurements. Scheme 3 illustrates the switching cycle mechanism for the bistable [2]catenanes [32–34]. In the neutral state, the CBPQT^{4+} ring resides preferentially on the TTF site (ground state). The oxidation of the TTF unit is accompanied by a rapidly driven shuttling of the CBPQT^{4+} ring to the DNP site. Upon reduction of the TTF site back to its charge-neutral state, the [2]catenane passes through a metastable state. The relaxation rate from this metastable state to the ground state (k in scheme 3) is typically too fast to be observed at room temperature in the solution phase. In the polymer environment, however, this relaxation is slowed down significantly [34], indicating that the mechanical movement of the CBPQT^{4+} ring

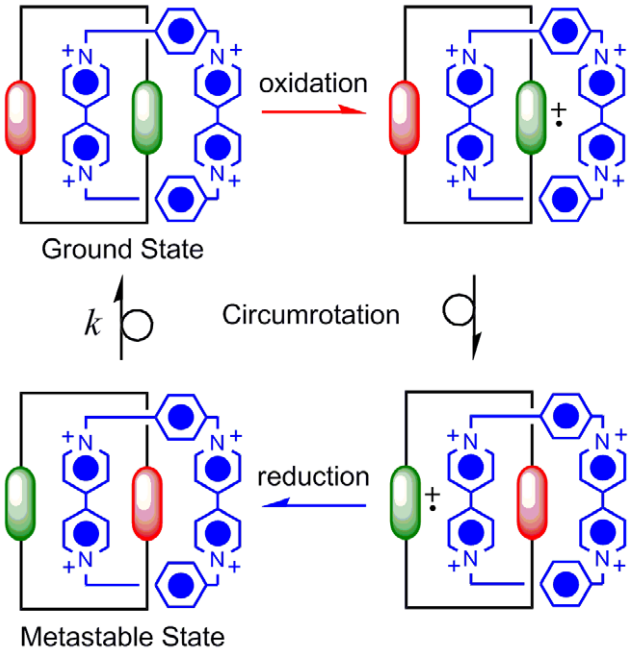

Scheme 3. The switching cycle for the bistable [2]catenanes, starting from the ground state (upper-left). The green and red sites on the ring components refer to the TTF and DNP binding sites, respectively. The metastable state (lower-left) is detectable in the polymer gel matrix.

is affected strongly by the viscosity of the medium [37, 38]. The $1/e$ decay time ($\tau = 1/k$) at room temperature of the two-station [2]catenanes $\mathrm{RG1}^{4+}$ and $\mathrm{RG2}^{4+}$ are 0.6 and 800 s, respectively [34]. This result means that we can control the colorimetric retention time by varying the molecular structure of the [2]catenanes.

8. Conclusions

Recent studies on electrochromic materials using inclusion complexes and mechanically interlocked molecules are summarized. We have already obtained the RGB colors from the inclusion complexes formed between $\mathrm{CBPQT}^{4+} \bullet 4\mathrm{PF}_6$ and DNP–TEG, TTF–TEG and DFBZ–TEG, respectively [35, 36]. The consistency between the association constants of the 1 : 1 complexes and the oxidation potentials for the π-electron donor units in a [2]catenane, incorporating DNP–C5DEG, TTF–TEG and DFBZ–TEG units in a macrocyclic polyether interlocked by a CBPQT^{4+} ring, has lead to the realization of an electrochemically controllable three-station [2]catenane [36]. With the combination of DNP–C5DEG, TTF–TEG, DFBZ–TEG, the station having the stronger affinity to $\mathrm{CBPQT}^{4+} \bullet 4\mathrm{PF}_6$ is oxidized at lower potential. In addition, we have already demonstrated electrochromic devices using the two-station [2]catenanes in polymer gel matrices [34].

In the case of the three-station [2]catenanes, we have not been able to confirm the RGB colors in the solution state, because the absorption bands of the oxidized TTF and BZ units screen the CT band between the CBPQT^{4+} and the recognition sites. This problem is one that we

believe can be solved in the fullness of time. In the case of the electrochromism in polymer gel matrices, the relaxation of the metastable sate to the ground state is much slower (about 2000 times) than that observed in the solution phase. Thus, the [2]catenane can exhibit the color of the CT band as long as it is in the metastable state. We are just starting to explore electrochromic materials using mechanically interlocked molecules. We have to make progress on a number of fronts simultaneously, including (i) colors, (ii) the binding strengths between the recognition sites and the $CBPQT^{4+}$ ring, (iii) the oxidation potential of the recognition sites, and (iv) the relaxation times from the metastable back to the ground states. An investigation of an incremental nature will lead ultimately to the development of the mechanically interlocked molecules in the field of the electrochromic devices.

Acknowledgments

This work was supported by the Microelectronics Advanced Research Corporation (MARCO) and its Focus Center on Functional Engineered Nano Architectonics (FENA), as well as the Defense Advanced Research Projects Agency (DARPA) and the Center for Nanoscale Innovative Defense (CNID).

References

[1] Nishikawa T and Mitani T 2003 *Sci. Technol. Adv. Mater.* **4** 81
[2] Tsukagoshi K, Iwao Y and Aoyagi Y 2006 *Sci. Technol. Adv. Mater.* **7** 231
[3] Weiser M 1991 *Sci. Am.* **265** 94
[4] Granmar M and Cho A 2005 *Science* **308** 785
[5] Comiskey B, Albert J D, Yoshizawa H and Jacobson J 1998 *Nature* **394** 253
[6] Rogers J A 2001 *Science* **291** 1502
[7] Huitema H E A, Gelinck G H, van der Putten J B P H, Kuijk K E, Hart C M, Cantatore E, Herwig P T, van Breemen A J J M and de Leeuw D M 2001 *Nature* **414** 599
[8] Luk Y-Y and Abbott N L 2003 *Science* **301** 623
[9] Anderson P, Nilsson D, Svensson P-O, Chen M, Malmström A, Remonen T, Kugler T and Berggren M 2002 *Adv. Mater.* **14** 1460
[10] Sonmez G, Sonmez H B, Shen C K F and Wudl F 2004 *Adv. Mater.* **16** 1905
[11] Deng W-Q, Flood A H, Stoddart J F and Goddard W A III 2005 *J. Am. Chem. Soc.* **127** 15994
[12] Sauvage J-P and Dietrich-Buchecker C O 1999 *Molecular Catenanes, Rotaxanes and Knots* (Weinheim: Wiley)
[13] Philp D and Stoddart J F 1991 *Synlett* 445
[14] Philp D and Stoddart J F 1996 *Angew. Chem. Int. Edn. Engl.* **35** 1154
[15] Stoddart J F and Tseng H-R 2002 *Proc. Natl. Acad. Sci. USA* **99** 4797
[16] Asakawa M *et al* 1999 *Eur. J. Org. Chem.* **985**
[17] Ballardini R, Balzani V, Fabio A D, Gandolfi M T, Becher J, Lau J, Nielsen M B and Stoddart J F 2001 *New J. Chem.* **25** 293
[18] Vignon S A, Wong J, Tseng H-R and Stoddart J F 2004 *Org. Lett.* **6** 1095
[19] Vignon S A and Stoddart J F 2005 *Collect. Czech. Chem. Commun.* **10** 1493
[20] Odell B, Reddington M V, Slawin A M Z, Spencer N, Stoddart J F and Williams D J 1988 *Angew. Chem. Int. Edn. Engl.* **27** 1547
[21] Brown C L, Philp D and Stoddart J F 1991 *Synlett* 462
[22] Asakawa M, Dehaen W, Lábbé G, Menzer S, Nouwen J, Raymo F M, Stoddart J F and Williams D J 1996 *J. Org. Chem.* **61** 9591
[23] Doddi G, Ercolani G, Mencarelli P and Piermattei A 2005 *J. Org. Chem.* **70** 3761
[24] Philp D, Slawin A M Z, Spencer N, Stoddart J F and Williams D J 1991 *J. Chem. Soc. Chem. Commun.* 1584
[25] Asakawa M, Ashton P R, Balzani V, Credi A, Mattersteig G, Matthews O A, Montalti M, Spencer N, Stoddart J F and Venturi M 1997 *Chem. Eur. J.* **3** 1992
[26] Nielsen M B, Jeppesen J O, Lau J, Lomholt C, Damgaard D, Jacobsen J P, Becher J and Stoddart J F 2001 *J. Org. Chem.* **66** 3559
[27] Reddington M V, Slawin A M Z, Spencer N, Stoddart J F, Vicent C and Williams D J 1991 *J. Chem. Soc. Chem. Commun.* 630
[28] Ashton P R, Philp D, Spencer N, Stoddart J F and Williams D J 1994 *J. Chem. Soc. Chem. Commun.* **4** 181
[29] Ashton P R *et al* 1997 *Chem. Eur. J.* **3** 152
[30] Córdova E, Bissell R A, Spencer N, Ashton P R, Stoddart J F and Kaifer A E 1993 *J. Org. Chem.* **58** 6440
[31] Córdova E, Bissell R A and Kaifer A E 1995 *J. Org. Chem.* **60** 1033
[32] Asakawa M *et al* 1998 *Angew. Chem. Int. Ed.* **37** 333
[33] Balzani V, Credi A, Mattersteig G, Matthews O A, Raymo F M, Stoddart J F, Venturi M, White A J P and Williams D J 2000 *J. Org. Chem.* **65** 1924
[34] Steuerman D W, Tseng H-R, Peters A J, Flood A H, Jeppesen J O, Nielsen K A, Stoddart J F and Heath J R 2004 *Angew. Chem. Int. Ed.* **43** 6486
[35] Ikeda T, Saha S, Aprahamian I, Leung K C-F, Williams A, Deng W-Q, Flood A H, Goddard W A III and Stoddart J F 2007 *Chem. Asian J.* **2** 76
[36] Ikeda T, Aprahamian I and Stoddart J F 2007 *Org. Lett.* **9** 1481
[37] Grote R F and Hynes J T 1980 *J. Chem. Phys.* **73** 2715
[38] Grote R F and Hynes J T 1981 *J. Chem. Phys.* **74** 4465